

Inactivation of ABL kinases suppresses non-small cell lung cancer metastasis

Jing Jin Gu,¹ Clay Rouse,² Xia Xu,¹ Jun Wang,¹ Mark W. Onaitis,^{3,4} and Ann Marie Pendergast¹

¹Department of Pharmacology and Cancer Biology, ²Division of Laboratory Animal Resources, ³Department of Surgery, Duke University School of Medicine, Durham, North Carolina, USA. ⁴Department of Surgery, University of California, San Diego, San Diego, California, USA.

Current therapies to treat non-small cell lung carcinoma (NSCLC) have proven ineffective owing to transient, variable, and incomplete responses. Here we show that ABL kinases, ABL1 and ABL2, promote metastasis of lung cancer cells harboring EGFR or KRAS mutations. Inactivation of ABL kinases suppresses NSCLC metastasis to brain and bone, and other organs. ABL kinases are required for expression of prometastasis genes. Notably, ABL1 and ABL2 depletion impairs extravasation of lung adenocarcinoma cells into the lung parenchyma. We found that ABL-mediated activation of the TAZ and β -catenin transcriptional coactivators is required for NSCLC metastasis. ABL kinases activate TAZ and β -catenin by decreasing their interaction with the β -TrCP ubiquitin ligase, leading to increased protein stability. High-level expression of ABL1, ABL2, and a subset of ABL-dependent TAZ- and β -catenin-target genes correlates with shortened survival of lung adenocarcinoma patients. Thus, ABL-specific allosteric inhibitors might be effective to treat metastatic lung cancer with an activated ABL pathway signature.

Introduction

Lung cancer is the leading cause of cancer mortality in the U.S., with an overall 5-year survival rate of ~15%. Non-small cell lung carcinoma (NSCLC) accounts for ~80% of all lung cancer cases and can be classified into adenocarcinoma (AC) (40%), squamous cell carcinoma (SCC) (30%), and large cell carcinoma (LCC) (15%) (1). Major drivers of lung AC include mutations of KRAS (~30%) and the epidermal growth factor receptor (EGFR) (10%–15%). However, the identities of the pathways that promote the progression of ~40% of AC, ~60% of SCC, and the majority of LCC tumors, are currently unknown (1). Current therapies against driver kinases including mutant EGFR have proven ineffective owing to variable, transient, and incomplete responses, and patients with KRAS-mutant lung cancer exhibit poor outcome and have few tractable therapeutic options (2).

Metastases are common and devastating complications of lung cancer linked to ~90% of lung cancer deaths (3), with ~65% of lung cancer patients presenting with metastasis at the time of diagnosis (4). Brain metastases can be found in 10% to 25% of lung cancer patients and are associated with unfavorable prognosis and loss of cognitive functions (5). Approximately 40% of NSCLC cases exhibit bone metastasis associated with severe pain and bone fracture. The mechanisms that drive NSCLC metastasis are poorly understood and thus greater mechanistic insights into this process are urgently needed to identify effective therapies.

ABL1 and *ABL2* were first identified as oncogenes in leukemias (6), but recent data generated from The Cancer Genome Atlas (TCGA) revealed alterations in *ABL2* and *ABL1* in lung cancer (7). Copy number enhancement of *ABL2* was reported in NSCLC cells sensitive to the SRC/ABL inhibitor dasatinib (8). Rare somatic mutations in *ABL1* have been reported in 1% to 2% of patients with lung AC, and 2 of the *ABL1* mutations identified were recently shown to confer sensitivity to the ATP-competitive inhibitors imatinib and dasatinib in lung cancer cell lines (9). However, activation of ABL kinases based on genomic alterations is likely to underestimate the involvement of these kinases in solid tumors because ABL proteins can be overexpressed and activated in the absence of gene amplification or increased mRNA levels (10). In this regard, increased ABL tyrosine phosphorylation, indicative of kinase activation, has been detected in lung cancer cells in the absence of *ABL1* and *ABL2* genomic alterations (11). To date no studies have directly evaluated the biological consequences of targeting the ABL kinases with specific allosteric inhibitors or

Conflict of interest: The authors have declared that no conflict of interest exists.

Submitted: July 19, 2016

Accepted: November 15, 2016

Published: December 22, 2016

Reference information:

JCI Insight. 2016;1(21):e89647.

doi:10.1172/jci.insight.89647.

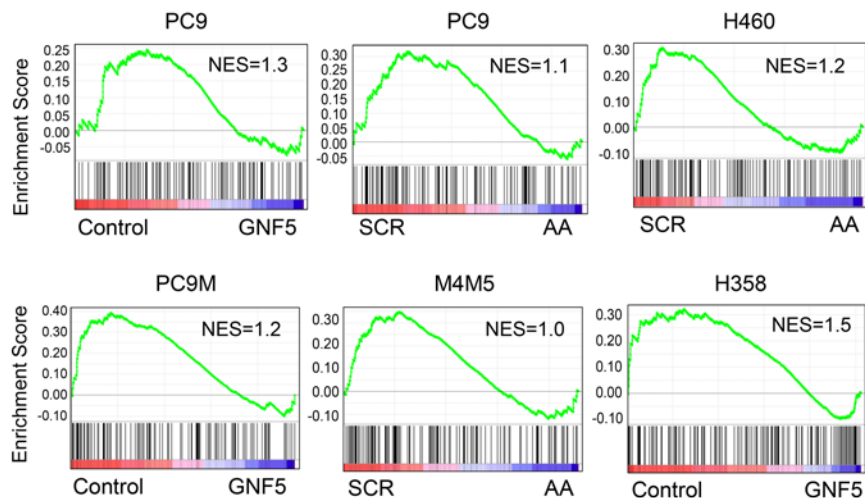


Figure 1. ABL kinases are required for expression of non-small cell lung carcinoma metastasis genes. Gene set enrichment analysis of metastasis signature genes using RNAseq data from the indicated lung cancer cell lines treated with or without the ABL kinase-specific allosteric inhibitor GNF5, or transduced with lentiviruses encoding either scrambled (SCR) or ABL1/ABL2-specific (AA) shRNAs. NES, normalized enrichment score.

genetic inactivation in mouse models of lung cancer, or examined whether ABL kinases have a role in lung cancer metastasis.

Here we identify a previously unappreciated role for the ABL kinases in promoting NSCLC metastasis in part by facilitating efficient tumor cell extravasation. Mechanistically, ABL kinases promote NSCLC metastasis

through posttranscriptional regulation of β -catenin and the Hippo pathway transcriptional coactivator TAZ. High-level expression of *ABL1* and *ABL2* together with selected downstream targets correlates with shortened survival by lung AC patients. Our findings suggest that ABL allosteric inhibitors might be employed for the treatment of metastatic NSCLC with an activated ABL pathway signature.

Results

ABL kinases promote expression of genes implicated in NSCLC metastasis and are required for NSCLC metastasis. A hallmark of lung cancer is the presence of metastases at the time or within a few months of diagnosis, and NSCLC metastasis has been linked to ~90% of lung cancer deaths (12). Thus, new therapies targeting molecules required for metastasis are needed for the treatment of lung cancer (13, 14). Although both *ABL1* and *ABL2* have been linked to NSCLC tumor growth in xenograft models (8, 9), little is known regarding the involvement of ABL kinases in lung cancer metastasis. We first evaluated whether *ABL1* and *ABL2* kinases regulate gene expression profiles linked to lung cancer metastasis, through analysis of the transcriptome of various NSCLC cell lines following inactivation of the ABL kinases using next-generation sequencing (RNAseq). Among NSCLC cell lines used were the EGFR-mutant PC9 cells established from a lymph node of a lung AC patient with an EGFR^{-Δexon19} mutation, as well as the KRAS mutant H358 and H460 lung cancer cells. We also employed the highly metastatic PC9M and M4M5 cell lines derived from parental PC9 and H460 cells, respectively (15–17). Both the PC9M and M4M5 cells display enhanced metastatic activity compared with parental cells. Gene set enrichment analysis (GSEA) (18) using multiple metastasis signature gene sets (15, 17, 19–22) was employed to query pathways dependent on the ABL kinases. NSCLC cells knocked down for both *ABL1* and *ABL2* or treated with the ABL allosteric inhibitor GNF5 displayed reduced expression of metastasis gene signatures (Figure 1). These data suggest that ABL kinases may promote signaling pathways required for NSCLC metastasis.

The presence of NSCLC metastases near the time of diagnosis suggests that lung cancer cells induce early activation of signaling pathways required not only for invasion by primary tumor cells, but also for subsequent steps in the metastatic cascade. To experimentally evaluate whether ABL kinases regulate steps in the metastatic cascade following invasion and intravasation, we employed intracardiac injection of scrambled shRNA-treated or *ABL1*/*ABL2* knockdown PC9 cells into immunodeficient mice. Lung cancer cells were engineered to express luciferase to monitor metastatic progression by bioluminescent imaging (BLI). Depletion of *ABL1* and *ABL2* in PC9 cells elicited a profound decrease in metastatic activity (Figure 2, A and B), which was accompanied by increased survival of mice inoculated with the *ABL1*/*ABL2* knockdown cells (Figure 2, C and D). Similarly, knockdown of the ABL kinases in the highly metastatic PC9M lung cancer cells resulted in decreased metastasis, with a corresponding increase in survival for mice injected with the ABL-deficient cells compared with control cells (Supplemental Figure 1, A–D; supplemental material available online with this article; doi:10.1172/jci.insight.89647DS1). To evaluate the specificity of the shRNAs, we evaluated the metastatic activity of PC9 cells transduced with a second set of shRNAs specific for *ABL1* and *ABL2*. Knockdown of *ABL1* and *ABL2* with the second

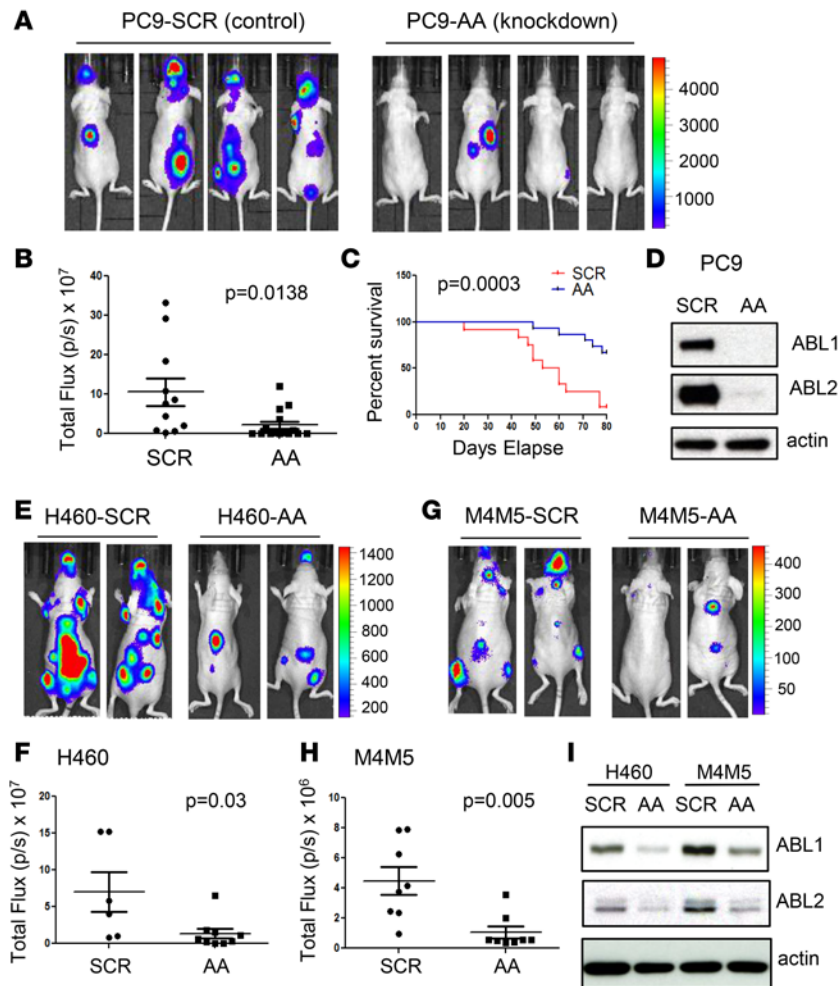


Figure 2. Depletion of ABL1 and ABL2 suppresses non-small cell lung carcinoma metastasis. (A)

PC9 cells labeled with luciferase were transduced with lentiviruses encoding either scrambled (SCR) or ABL1/ABL2-specific (AA) shRNAs, and cells were delivered by intracardiac injection into nude mice. Tumor metastasis was detected by bioluminescent imaging (BLI). Representative images at day 28 are shown. (B) BLI counts (in photons per second [p/s]) of each individual mouse for the indicated groups (SCR $n = 11$, AA $n = 15$). (C) Percentage of mice surviving over the indicated times (days). (D) Depletion of ABL1 and ABL2 proteins was confirmed by Western blotting. (E) Luciferase-labeled H460 cells transduced with either SCR or AA shRNAs were delivered by intracardiac injection into nude mice. Representative metastasis images at day 12 are shown. (F) BLI counts of each mouse for the indicated groups (SCR $n = 6$, AA $n = 9$). (G) M4M5 cells transduced with either SCR or AA shRNAs were intracardiac injected into nude mice. Representative metastasis images at day 14 are shown. (H) BLI counts of each mouse for the indicated groups ($n = 8$ for each group). (I) Depletion of ABL1 and ABL2 proteins in H460 and M4M5 cells was confirmed by Western blotting. Data are represented as mean \pm SEM. All P values were determined by Student's t test or log-rank test.

set of shRNAs markedly decreased metastatic activity to levels comparable to that elicited by the first set of ABL1/ABL2-specific shRNAs (Supplemental Figure 1, E–G).

To evaluate whether ABL kinases might be required for metastasis of lung cancer types harboring distinct oncogenic drivers other than mutant EGFR, we employed the H460 lung

cancer cells harboring mutant KRAS and the highly metastatic H460-derived M4M5 cells (Figure 2, E–I). Knockdown of both ABL1 and ABL2 elicited a profound loss of metastatic activity by both H460 parental (Figure 2, E and F) and M4M5 cells (Figure 2, G and H). NSCLC cells metastasized primarily to brain and bone, but also to lung, spleen, and kidney (Supplemental Figure 2), and inhibition of the ABL kinases suppressed metastasis to these sites. Thus, ABL kinases promote metastasis by lung cancer cells driven by EGFR or KRAS mutations.

Allosteric inhibition of the ABL kinases suppresses NSCLC metastasis. To evaluate whether inhibiting the enzymatic activity of the ABL kinases could suppress lung cancer metastasis, we employed GNF5, a compound that targets the unique ABL myristate-binding site and that functions as an allosteric inhibitor for the ABL family kinases (23). We employed the ABL allosteric inhibitor rather than the ATP-competitive inhibitors imatinib (STI571/Gleevec), nilotinib, or dasatinib because the ATP-competitive inhibitors target multiple kinases in addition to the ABL kinases (6). Further, we found that the ATP-competitive inhibitors imatinib and nilotinib, but not the GNF5 allosteric inhibitor, induced ERK activation in diverse lung cancer cells (Supplemental Figure 3A). All 3 compounds inhibited the endogenous ABL kinases as measured by decreased phosphorylation of the ABL substrate CrkL on tyrosine 207 (Supplemental Figure 3A). These findings are consistent with previous reports showing that the ATP-competitive inhibitors imatinib, nilotinib, and dasatinib elicit activation of the RAF/ERK pathway in various cancer cell types (24). Importantly, administration of GNF5 by oral gavage was well tolerated and did not induce weight loss in mice (Supplemental Figure 3B). Mice treated with GNF5 following inoculation with the highly metastatic PC9M (Figure 3, A and B) and M4M5 (Figure 3, C and D) cells exhibited markedly decreased metastasis compared with control vehicle-treated mice. The ABL allosteric inhibitor decreased metastasis regardless of whether the mice were treated with GNF5 one day after intracardiac injection of PC9M cells (Figure 3, A and B) or 8 days after injection of M4M5 cells

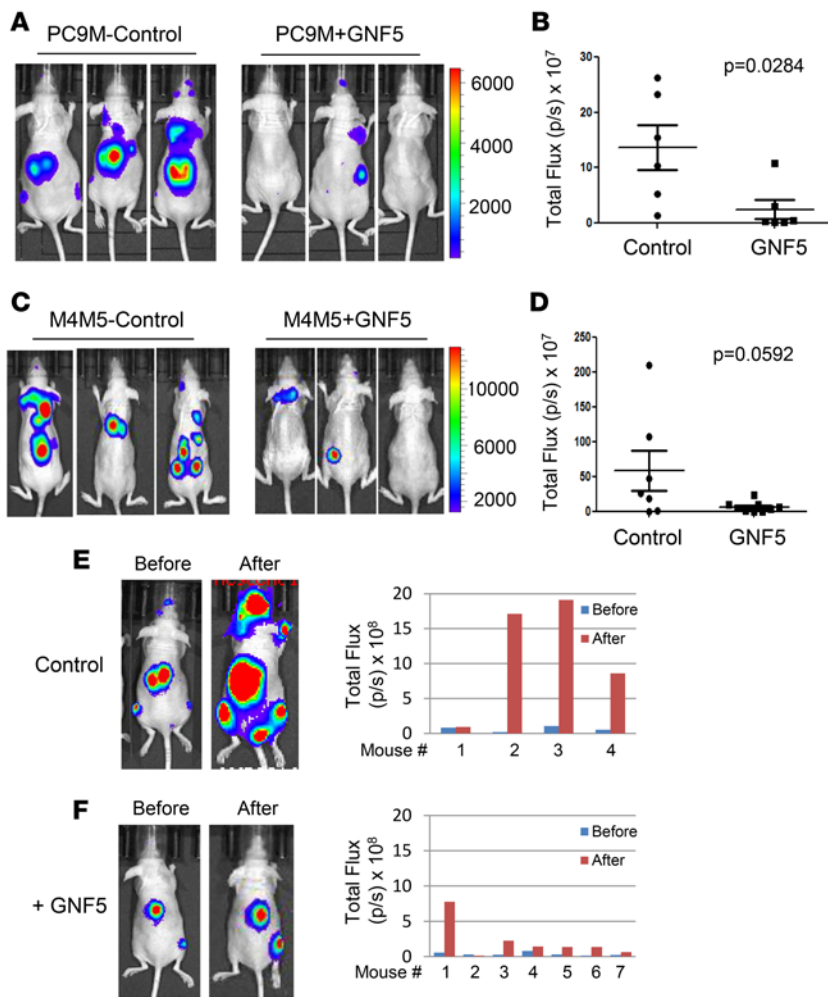


Figure 3. Inhibition of ABL kinase activity suppresses non-small cell lung carcinoma metastasis. (A) PC9M cells labeled with luciferase were delivered by intracardiac injection into nude mice. Mice were treated 1 day after injection with or without GNF5 at 100 mg/kg by oral gavage twice per day. Representative images taken at day 18 are shown. (B) Bioluminescent imaging (BLI) counts (in photons per second [p/s]) of each mouse for the indicated groups ($n = 6$ each group). (C) M4M5 cells labeled with luciferase were delivered by intracardiac injection into nude mice. Mice were treated 8 days after injection with or without GNF5 at 50 mg/kg by intraperitoneal injection once per day. Representative images at 12 days after GNF5 treatment are shown. (D) BLI counts of each mouse for the indicated groups (control, $n = 7$, GNF5 $n = 9$). Data are represented as mean \pm SEM. All P values were determined by Student's t test. (E and F) Luciferase-labeled PC9M cells were delivered by intracardiac injection into nude mice. After 10 days, mice bearing metastatic tumors were divided into 2 groups, and treated with vehicle (E) or GNF5 (F) by oral gavage for 14 days. Representative BLI images (left); BLI counts of each individual mouse before and after treatment for the indicated groups (right). Control $n = 4$, GNF5 treated $n = 7$.

(Figure 3, C and D). Further, GNF5 treatment of mice with established metastatic tumors following detection by BLI showed that the ABL allosteric inhibitor also effectively inhibited the growth of well-established PC9M metastatic lesions (Figure 3, E and F). Together these data demonstrate that allosteric inhibition of ABL kinases is an effective therapeutic strategy to suppress multiple-organ metastasis by lung cancer cells.

ABL kinases are required for NSCLC cell extravasation into the lung parenchyma. A limiting step in the metastatic cascade is extravasation, the ability of cancer cells to exit the circulation and transverse the vasculature in order to initiate metastatic seeding and colonization (13, 25). Thus, we evaluated whether ABL kinases were required for efficient lung cancer cell extravasation by injecting PC9 cells into the mouse tail vein, and quantifying the number of extravasated cancer cells in the lung parenchyma 24 hours after injection, a time point when cancer cells are extravascular but have not yet replicated. We found that knockdown of ABL1 and ABL2 with 2 different sets of ABL1/ABL2-specific shRNAs markedly decreased extravasation by PC9 (Figure 4, A–D) and PC9M (Supplemental Figure 4, A and B) lung AC cells. Interestingly, mice injected with ABL1/ABL2 knockdown cells exhibited decreased numbers of extravasated PC9 circulating tumor cell (CTC) clusters, which were predominantly detected in mice injected with control PC9 cells (Figure 4C). CTC clusters were reported to have increased metastatic potential compared with single tumor cells (26). Notably, depletion of the ABL kinases did not decrease PC9 cell numbers in pulmonary blood vessels observed at 2 hours after tail vein injection and prior to extravasation (Supplemental Figure 4, C and D). These data show that ABL kinases are required for efficient dissemination of NSCLC cells into the lung parenchyma, and suggest that impaired metastasis by lung cancer cells lacking ABL kinases may be mediated in part by decreased extravasation.

To further investigate whether inactivation of the ABL kinases affects lung cancer cell growth and survival, we examined cell proliferation and survival with CellTiter-Glo and anchorage-independent colony formation assays (Supplemental Figure 5, A–D). Depletion of ABL kinases in PC9, PC9M, and H460 cells did not affect 2-dimensional cell growth and viability (Supplemental Figure 5, A and B). However, depletion of ABL1 and ABL2, or pharmacological inhibition of ABL kinase activity, markedly decreased 3D anchorage-independent growth (Supplemental Figure 5, C and D). Moreover, doxycycline-

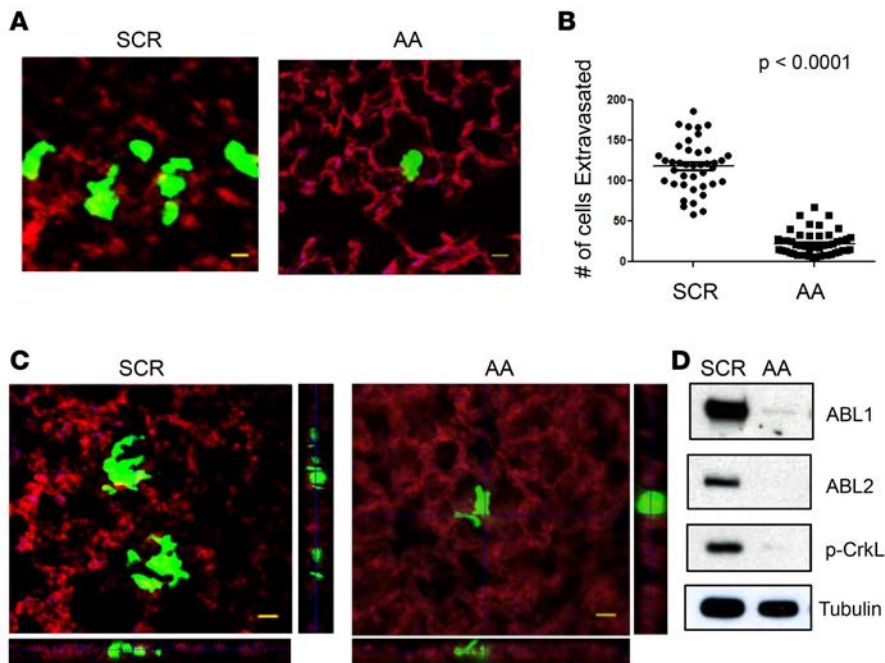


Figure 4. ABL kinases promote tumor cell extravasation into the lung parenchyma. (A) PC9 cells transduced with lentiviruses encoding either scrambled (SCR) or ABL1/ABL2-specific (AA) shRNAs were labeled with CellTracker Green and then injected into nude mice through the tail vein. Lung vessels were stained with rhodamine-conjugated lectin by tail vein injection 5 minutes before sacrificing mice. Lung cancer cells extravasated into the lung were counted 24 hours after injection. Representative images are shown. (B) Quantification of extravasated PC9 cells in the lungs (150- μ m sections, $n = 10$ for each mouse) for indicated mice (SCR $n = 4$, AA $n = 5$). Data are represented as mean \pm SEM. The P values were determined by Student's t test. (C) Clusters of lung cancer cells extravasated into the lung parenchyma were imaged to visualize orthogonal views. Representative images are shown. (D) Depletion of ABL1 and ABL2 proteins was confirmed by Western blotting; p-CrkL is indicative of ABL kinase activity. All scale bars: 20 μ m.

inducible knockdown of ABL1 profoundly inhibited the growth of H460 xenografts (Supplemental Figure 5, E–H). Thus, ABL kinases may promote lung cancer cell growth and viability depending on the cellular context and surrounding microenvironment (blood vessel versus lung parenchyma).

ABL kinases regulate WNT and TAZ signaling networks in NSCLC cells. To investigate the mechanisms by which ABL kinases promote NSCLC metastasis, we carried out GSEA of the altered transcriptome induced by inactivation of the ABL kinases in PC9, PC9M, and H358 NSCLC cells. We found that pharmacological inhibition or knockdown of the ABL kinases markedly reduced the WNT/ β -catenin (Figure 5A and Supplemental Figure 6A) and TAZ (Figure 5B and Supplemental Figure 6B) pathway signatures (18, 27, 28).

Both the WNT/ β -catenin and Hippo/TAZ pathways have been independently implicated in lung cancer progression (29–31). We found that whereas pharmacological inhibition or depletion of the ABL kinases did not significantly affect mRNA expression of *TAZ* (encoded by the *WWTR1* gene) and β -catenin (encoded by the *CTNNB1* gene) (Supplemental Figure 6C), inhibition of the ABL kinases in multiple NSCLC cell lines decreased expression of WNT/ β -catenin targets *TCF4* and *EDN1* (endothelin 1), and markedly reduced the transcription of the TAZ target gene *CTGF* (connective tissue growth factor) (Supplemental Figure 6D). Further, pharmacological inhibition of the ABL kinases decreased the transcriptional activity of the endogenous β -catenin and TAZ coactivators measured with the β -catenin–responsive luciferase reporter (7x Tcf-FFluc) (Figure 5C) and the TAZ-responsive luciferase reporter (8x GTIIC lux) (Figure 5D). Notably, inhibition of ABL kinase activity with GNF5 or ABL1/ABL2 knockdown decreased the abundance of β -catenin and TAZ proteins (Figure 5E). Conversely, expression of a constitutively active form of ABL2 (ABL2-PP) enhanced protein abundance of TAZ and β -catenin (Figure 5E).

Canonical WNT signaling promotes β -catenin protein stabilization, nuclear translocation, and association with the DNA-binding TCF/LEF transcription factors to drive expression of target genes (32). We found that WNT3A-induced nuclear translocation of both β -catenin and TAZ was inhibited by treatment of PC9 cells with the GNF5 allosteric inhibitor, as detected by Western blotting of nuclear and cytosolic fractions (Figure 5F). TAZ transcriptional activation can be induced by factors such as lysophosphatidic acid (LPA) that activate G-protein-coupled receptors. Recently, TAZ activation was reported to occur downstream of noncanonical WNT signaling through binding to the Frizzled/ROR receptor complex (33). To evaluate whether ABL kinases regulate the abundance of proteins targeted by β -catenin and TAZ signaling, PC9 (Figure 5, G and H) and H460 (Figure 5I) cells were stimulated with WNT3A for activation of both WNT and TAZ signaling, or LPA to induce TAZ activation. Treatment with GNF5 or knockdown

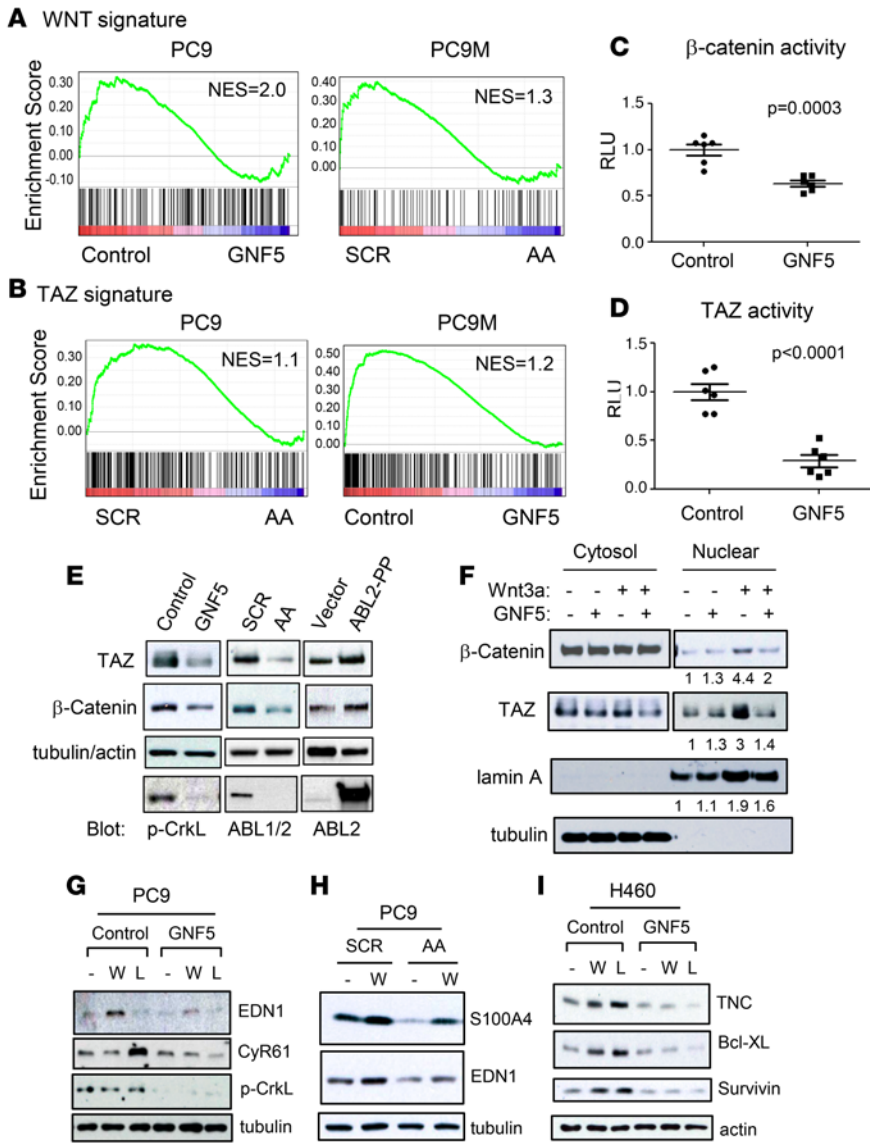


Figure 5. ABL kinases promote β -catenin and TAZ protein abundance, nuclear translocation, and downstream signaling. (A and B) Gene set enrichment analysis of WNT (A) and TAZ (B) signature genes using RNAseq data from PC9 and PC9M cells treated with or without GNF5 or transduced with either scrambled (SCR) or ABL1/ABL2-specific (AA) shRNAs as indicated. (C and D) Endogenous β -catenin (C) and TAZ (D) activities in PC9 cells with or without GNF5 treatment was analyzed using luciferase-reporter assays and normalized to β -galactosidase activity. Data are represented as mean \pm SEM. The *P* values were determined by Student's *t* test (control *n* = 6, GNF5 *n* = 6). (E) PC9 cells were treated with or without GNF5 (left panel), transduced with either SCR or AA shRNAs (middle panel), or transduced with either vector control or active ABL2 (ABL2-PP, right panel). Western blots were probed with the indicated antibodies. (F) PC9 cells were pretreated with or without GNF5 for 1 hour followed by stimulation with WNT3A (100 ng/ml) for 5 hours. Cell lysates were fractionated into cytosolic and nuclear fractions, and TAZ and β -catenin localization was probed by Western blotting. For cytosolic β -catenin and TAZ samples, shorter exposure times are shown. Lamin A (nuclear marker) and tubulin (cytosolic marker) were used to assess the purity of the fractionation procedure. The nuclear fraction was quantified using Fiji ImageJ software. Relative protein intensity is shown. (G–I) PC9 cells pretreated with or without GNF5 for 1 hour (G) or transduced with SCR or AA shRNAs (H) and H460 cells pretreated with or without GNF5 for 1 hour (I) were stimulated without (–) or with WNT3A (W, 100 ng/ml) for 5 hours or LPA (L, 1 μ M) for 4 hours. WNT and TAZ downstream target proteins were analyzed by Western blotting with the indicated antibodies. Samples were run contemporaneously in several parallel gels. EDN1, CyR61, and TNC proteins were analyzed from the culture supernatant. ABL kinase activity was detected by blotting for p-CrkL; tubulin and actin were used as loading controls.

of ABL proteins in ligand-stimulated cells decreased the abundance of WNT/ β -catenin downstream targets, including EDN1 and S100A4, as well as TAZ downstream targets, including TNC, CyR61, survivin, and Bcl-XL (Figure 5, G–I). Together these data reveal a role for the ABL kinases in promoting TAZ and β -catenin protein abundance, nuclear translocation, and transcriptional activity leading to activation of corresponding downstream targets.

ABL kinases regulate β -catenin and TAZ protein stability. The stability of both β -catenin and TAZ proteins is regulated by the β -TrCP E3 ubiquitin ligase (34). To evaluate whether the decreased abundance of TAZ and β -catenin in NSCLC cells lacking ABL kinases was due to reduced protein stability, we employed the proteasome inhibitor MG132. Treatment with MG132 reversed the reduction of TAZ and β -catenin protein levels induced by inhibition of the ABL kinases (Figure 6A). Moreover, treatment of PC9 parental cells and PC9 cells expressing constitutively active ABL1 (ABL1-PP) with cycloheximide (CHX) to inhibit the synthesis of new proteins revealed that whereas endogenous TAZ and β -catenin protein levels decreased over time in the presence of CHX in control cells, both TAZ and β -catenin proteins were stable in cells expressing active ABL1-PP (Figure 6B). Conversely, inhibition of ABL kinases with GNF5 markedly enhanced TAZ protein degradation in the presence of CHX compared with control cells (Supplemental Figure 7, A and B). Together these data support a role for ABL kinases in posttranscriptional regulation of β -catenin and TAZ protein stability.

Canonical WNT signaling inhibits β -catenin phosphorylation by GSK3 (on S33, S37, and T41) and CK1 (on S45), thereby preventing binding to the β -TrCP E3 ubiquitin ligase that targets β -catenin for

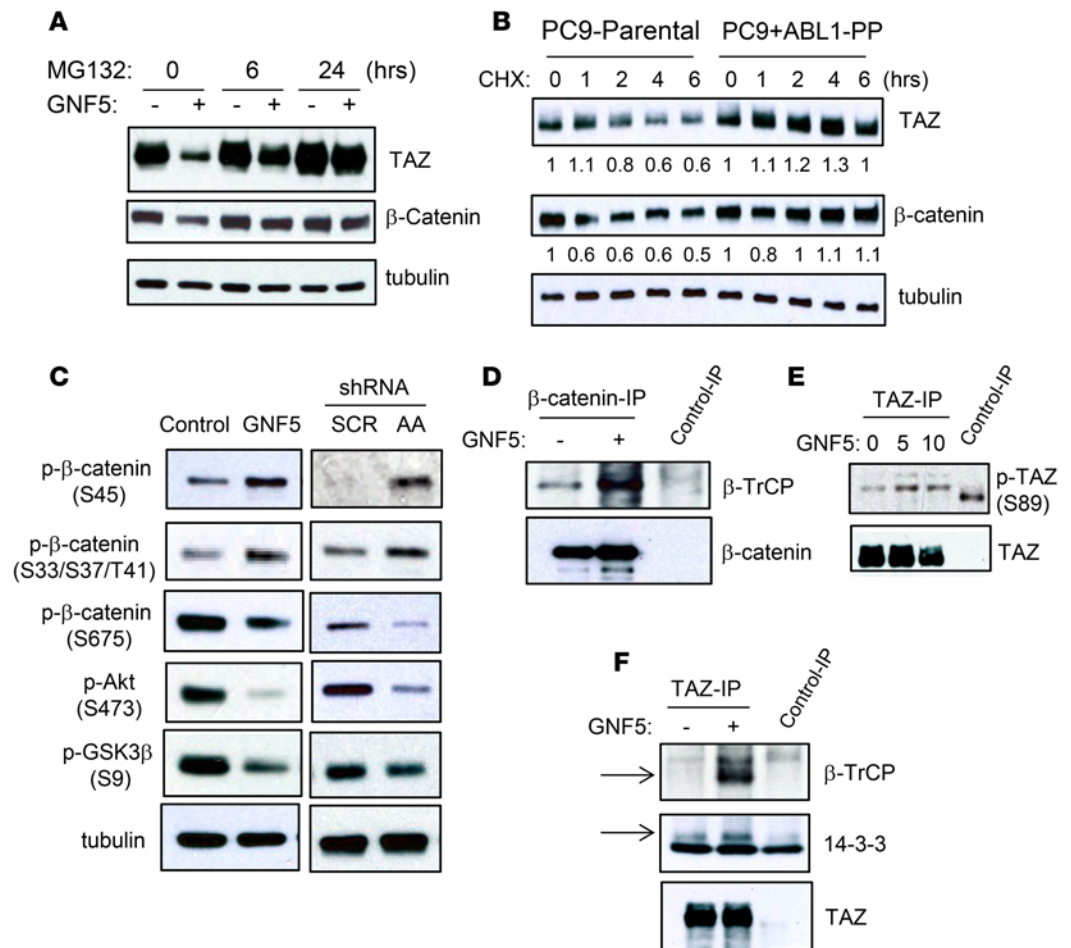


Figure 6. ABL kinases promote TAZ and β -catenin protein stability. (A) PC9 cells were treated with or without GNF5 followed by addition of MG132 (10 μ M for 6 hours, 1 μ M for 24 hours). TAZ and β -catenin protein levels were evaluated by Western blotting. Tubulin was used as loading control. (B) PC9 parental or PC9 cells expressing active ABL1 (ABL1-PP) were treated with cycloheximide (CHX, 100 μ g/ml) for the indicated times. Expression of TAZ and β -catenin proteins was analyzed by Western blotting and quantified using Fiji ImageJ software. Relative protein intensity is shown. The membrane was stripped and reprobed with anti-tubulin antibody. (C) PC9 cells were treated with or without GNF5 (left panel), or transduced with either scrambled (SCR) or ABL1/ABL2-specific (AA) shRNAs (right panel). Cell lysates were analyzed by Western blotting with antibodies specific for phosphorylated serine (S) or threonine (T) residues in β -catenin (p- β -catenin), GSK3 β (p-GSK3 β), and Akt (p-Akt). Tubulin was used as loading control. The same samples were run contemporaneously in several parallel gels to blot with indicated antibodies. (D) PC9 cells were treated with or without GNF5 (24 hours); β -catenin protein was immunoprecipitated (IP) followed by Western blotting with anti- β -TrCP and reprobed with anti- β -catenin antibodies. (E) PC9 cells were treated with or without GNF5 in the indicated doses (μ M) for 48 hours. IP-TAZ was followed by Western blotting with anti-p-YAP (S127) for detecting p-TAZ S89 and reprobed with anti-TAZ antibody. (F) PC9 cells were treated with or without GNF5 (24 hours); IP-TAZ was followed by Western blotting with anti- β -TrCP and anti-14-3-3 antibodies and reprobed with anti-TAZ antibodies. Normal mouse IgG was used for control IPs.

degradation. The nonphosphorylated β -catenin dissociates from the destruction complex (APC, axin, GSK3, CK1, β -TrCP), and translocates to the nucleus to drive expression of target genes (32). In contrast with the inhibitory sites, phosphorylation of β -catenin on S675 by protein kinase A (PKA) promotes β -catenin nuclear accumulation and transcriptional activity (35). We found that phosphorylation of β -catenin on S45, S33/37, and T41 was markedly increased, and phosphorylation of β -catenin on S675 was decreased, upon pharmacological inhibition of the ABL kinases or depletion of ABL1/ABL2 proteins in PC9 cells (Figure 6C). The activation state of GSK3 β is negatively regulated by AKT-dependent phosphorylation of serine-9 (S9) on GSK3 β (36). We found that inactivation of the ABL kinases resulted in decreased phosphorylation of AKT on S473, which is indicative of reduced AKT activity, as well as reduced phosphorylation of GSK3 β on

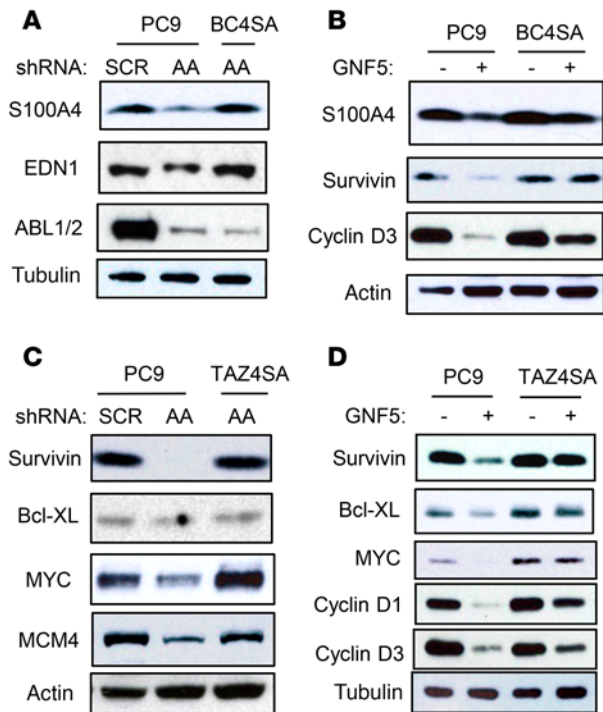
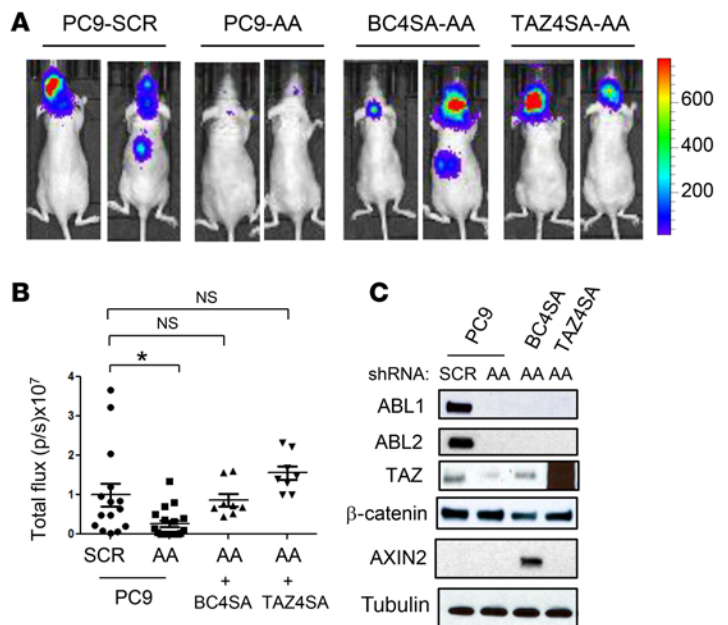


Figure 7. Activated forms of β -catenin and TAZ rescue the expression of downstream targets in lung cancer cells lacking ABL kinases. (A and B) PC9 parental or PC9 cells expressing activated β -catenin (BC4SA) were transduced with lentiviruses encoding either scrambled (SCR) or ABL1/ABL2-specific (AA) shRNAs (A) or treated with or without GNF5 (B). (C and D) PC9 parental or PC9 cells expressing activated TAZ (TAZ4SA) were transduced with either SCR or AA shRNAs (C) or treated with or without GNF5 (D). WNT or TAZ downstream target proteins were analyzed by Western blotting with the indicated antibodies. EDN1 was analyzed from the culture supernatant. Actin and tubulin were used as loading controls. The same samples were run contemporaneously in several parallel gels to blot with indicated antibodies.

S9 (Figure 6C). Conversely, expression of constitutively active forms of the ABL kinases, ABL1-PP and ABL2-PP, decreased phosphorylation of β -catenin on S33/S37/T41 and S45, sites that are required for recruitment to the destruction complex and degradation by the proteasome (Supplemental Figure 7C). Increased expression of activated ABL kinases enhanced the phosphorylation on GSK3 β -S9, leading to impaired GSK3 β kinase activity (Supplemental Figure 7C). Further, association of β -catenin with the β -TrCP E3 ubiquitin ligase was increased in cells treated with ABL allosteric inhibitor (Figure 6D). Together these data support a role for ABL kinases in promoting β -catenin protein stability through the AKT/GSK3 β kinase axis, and suggest that inhibition of the ABL kinases might be an effective strategy for inactivation of β -catenin signaling in lung cancer cells.

Like β -catenin, TAZ protein stability is regulated by the β -TrCP E3 ligase. Cells with active Hippo signaling kinases LATS1/2 promote phosphorylation of TAZ (on S66, S89, S117, and S311) leading to β -TrCP-mediated TAZ degradation (37). Additionally, phosphorylation of TAZ on S89 by LATS promotes cytoplasmic retention by binding to 14-3-3 proteins (38). Other kinases including GSK3 have been shown to phosphorylate TAZ and promote its degradation (39). We found that inhibition of ABL kinase activity increased TAZ phosphorylation on S89 (Figure 6E). Conversely, expression of constitutively active forms of the ABL kinases decreased phosphorylation of TAZ on S89 (Supplemental Figure 7D). We were unable to detect consistent ABL-dependent changes in the activity of the LATS Hippo pathway kinases known to phosphorylate TAZ on serine sites. However, we detected enhanced interaction between cytosolic TAZ with the β -TrCP E3 ligase and 14-3-3 protein in the presence of the ABL allosteric inhibitor (Figure 6F). Thus, inhibition of ABL kinases with

Figure 8. Activated forms of β -catenin and TAZ rescue metastasis in lung cancer cells lacking ABL kinases. (A) PC9 or PC9 cells expressing activated β -catenin (BC4SA) or activated TAZ (TAZ4SA) were transduced with lentiviruses encoding either scrambled (SCR) or ABL1/ABL2-specific (AA) shRNAs and cells were delivered by intracardiac injection into nude mice. Representative images are shown for indicated groups. (B) Bioluminescent imaging counts (in photons per second [p/s]) for each group are shown (SCR $n = 16$, AA $n = 18$, BC4SA-AA $n = 8$, TAZ4SA-AA $n = 8$). Data are represented as mean \pm SEM; P values were calculated using 1-way ANOVA followed by Tukey's honest significant difference test. * $P < 0.05$; NS, not significant. (C) Depletion of ABL1 and ABL2 and overexpression of TAZ4SA and BC4SA proteins was confirmed by Western blotting with the indicated antibodies. Activation of the β -catenin pathway was assessed by blotting for AXIN2. The same samples were run contemporaneously in several parallel gels to blot with indicated antibodies.



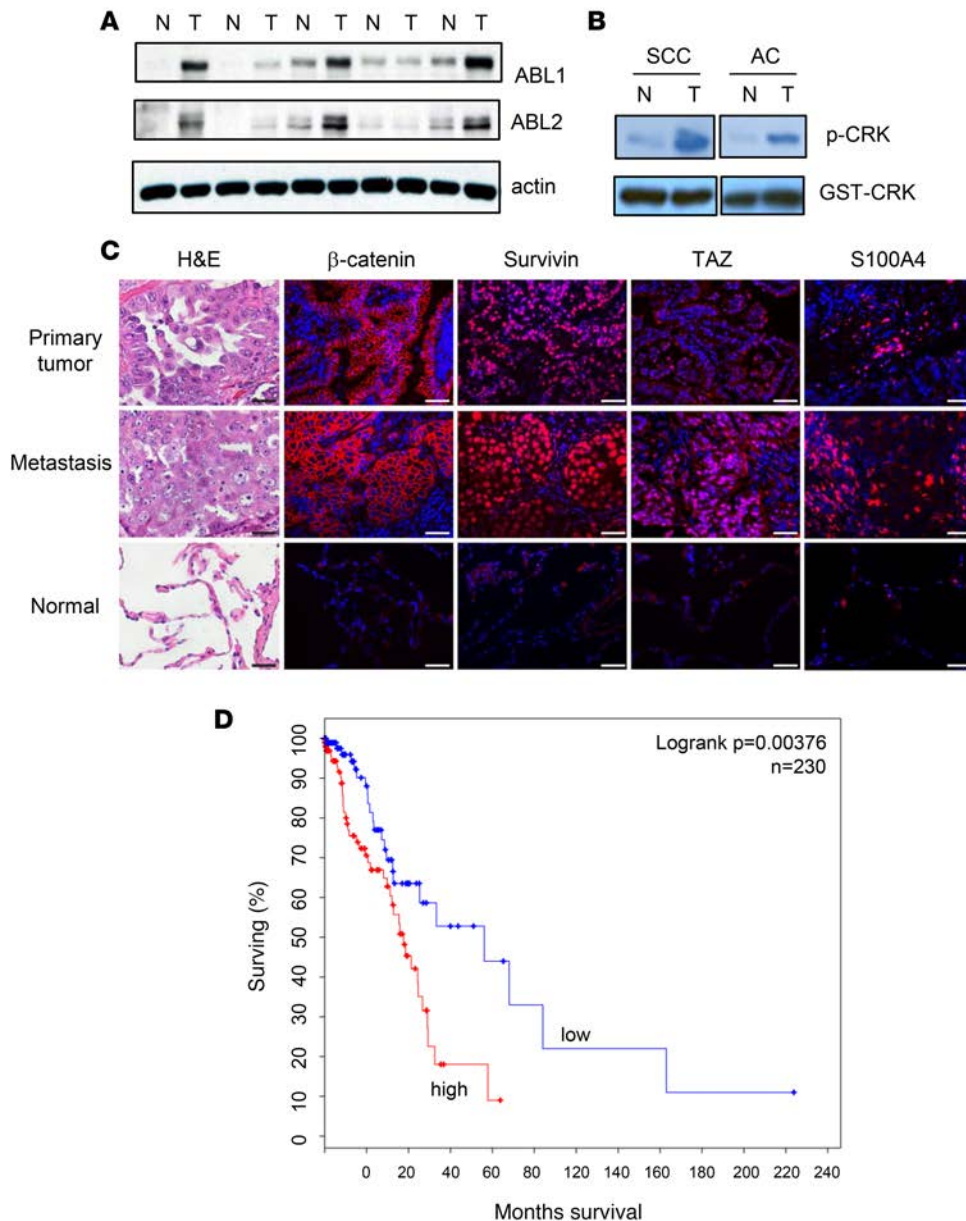


Figure 9. ABL kinases and downstream targets are upregulated and activated in non-small cell lung carcinoma (NSCLC) primary tumors and metastases. (A) Five pairs of primary human lung tumors (T) and adjacent normal tissue (N) were evaluated for ABL1 and ABL2 protein expression by Western blotting. Actin was used as loading control. (B) ABL proteins were immunoprecipitated and incubated with glutathione S-transferase-tagged CRK in an in vitro kinase assay. SCC, squamous cell carcinoma; AC, adenocarcinoma. Phosphorylation of CRK was evaluated using a phospho-specific (Y221) antibody. (C) NSCLC primary tumors and metastases specimens were analyzed with normal lung tissues by H&E and immunofluorescence staining with the indicated antibodies. Scale bars: 50 μ m. (D) Kaplan-Meier representation of overall survival based on the The Cancer Genome Atlas dataset with 230 lung adenocarcinoma patients according to high versus low expression of ABL1, ABL2, WWTR1 (TAZ), CTNNB1 (β -catenin), EDN1 (endothelin 1), S100A4, BCL2L1 (Bcl-XL), and BIRC5 (survivin) genes; P values were derived by the log-rank test.

GNF5 results in decreased overall TAZ protein levels and reduced TAZ nuclear localization in lung cancer cells. Together these findings show that active ABL kinases disrupt site-specific inhibitory phosphorylation of both TAZ and β -catenin, which in turn increase TAZ and β -catenin protein stability and enhance their nuclear coactivator functions.

Activation of β -catenin and TAZ signaling rescues expression of downstream targets and metastasis by lung cancer cells lacking ABL kinases. To evaluate whether β -catenin and TAZ are required downstream of the ABL kinases to promote NSCLC metastasis, activated forms of β -catenin (BC4SA: alanine substituted for S33, S37, T41, and S45) and TAZ (TAZ4SA: alanine substituted for S66, S89, S311, and 314) were expressed in PC9 cells lacking functional ABL kinases. Expression of BC4SA rescued the expression of downstream WNT signaling target proteins including S100A4, EDN1, survivin, and cyclin D3 in PC9 cells lacking ABL1 and ABL2 proteins or treated with the ABL kinase inhibitor (Figure 7, A and B; Supplemental Figure 8, A and B). Expression of active TAZ4SA rescued expression of downstream TAZ signaling targets including survivin, Bcl-XL, MYC, MCM4, cyclin D1, and cyclin D3 in PC9 cells lacking ABL1 and ABL2 or treated with the ABL kinase inhibitor (Figure 7, C and D; Supplemental Figure 8, C and D). Immunofluorescence staining revealed that the activated BC4SA and TAZ4SA proteins localized predominantly to the nucleus (Supplemental Figure 8E). Expression of BC4SA or TAZ4SA partially rescued colony formation in PC9 cells lacking active ABL kinases (Supplemental Figure 8, F and G). Importantly, expression of active BC4SA or TAZ4SA rescued metastatic activity of lung cancer cells lacking ABL1 and ABL2 (Figure 8, A–C). Together these findings demonstrate that ABL kinases promote NSCLC metastasis through the

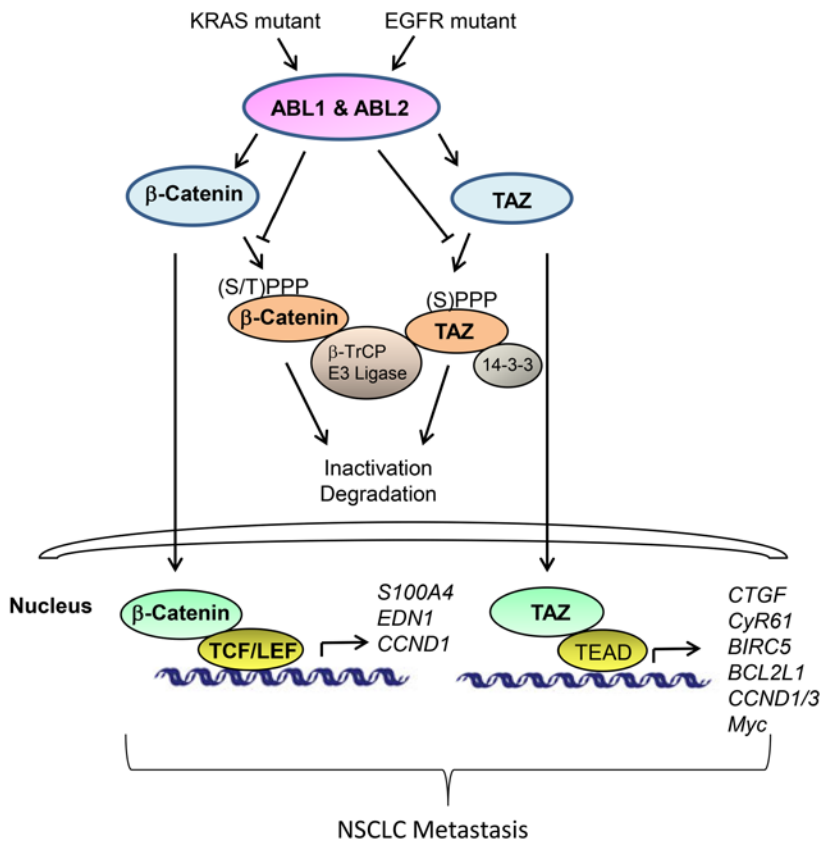


Figure 10. Proposed model for the role of ABL kinases in promoting lung cancer metastasis. Active ABL kinases in lung cancer cells harboring mutant KRAS or EGFR promote metastasis by enhancing β -catenin and TAZ protein stability and downstream signaling, leading to increased expression of genes required for non-small cell lung carcinoma (NSCLC) metastasis.

activation of WNT/ β -catenin and TAZ signaling pathways in mouse models.

To ascertain whether ABL kinases play a role in human lung cancer, we evaluated ABL1 and ABL2 protein abundance in 5 pairs of available NSCLC tumors and corresponding normal lung tissue. We found markedly increased expression of ABL1 and ABL2 kinases in 3 of the NSCLC tumor specimens compared with adjacent normal tissue from the same patient (Figure 9A). Further, increased ABL kinase activity was detected in lung AC and SCC tumors compared with adjacent normal lung (Figure 9B). To investigate whether the ABL pathway targets TAZ and β -catenin and their downstream transcriptional targets exhibit altered expression in human primary lung tumors and metastases, we analyzed a set of human lung AC patient specimens with or without KRAS mutations by immunofluorescence staining (Figure 9C and Supplemental Table 1).

We found that primary lung AC tumor specimens express higher levels of TAZ, β -catenin, survivin, and S100A4 compared with normal lung tissues (Figure 9C and Supplemental Table 1). Notably, higher levels of these ABL-pathway targets were detected in metastases isolated from lymph nodes compared with the primary lung AC tumors (Figure 9C and Supplemental Table 1). Activation of ABL family kinases in lung cancer specimens is consistent with the presence of genomic alterations of *ABL1* (8%) and *ABL2* (17%) that include amplification, mutation, and increased mRNA expression in a subset of NSCLC patients as reported in published datasets from TCGA (7). Using the same TCGA database, we found that while NSCLC AC patient survival is not significantly correlated with increased expression levels of TAZ or β -catenin alone, expression of the validated ABL-dependent gene signature (*ABL1*, *ABL2*, *TAZ*, *CTNNB1*, *EDN1*, *S100A4*, *BCL2L1*, and *BIRC5*) correlated with significantly decreased overall survival (Figure 9D). Overall our findings support a model where ABL kinases promote NSCLC metastasis in part by stabilization and activation of WNT/ β -catenin and TAZ signaling pathways, which lead to increase expression of targeting proteins critical for the metastasis (model Figure 10).

Discussion

A major challenge in the treatment of NSCLC is the presence of metastatic disease at the time of diagnosis. Rapid metastatic dissemination of lung cancer is likely dependent on the early activation of signaling networks that confer the capacity for cancer cells to migrate across the vascular endothelium, initiate metastatic seeding, and colonize distant organs. Here we uncovered a role for ABL kinases in promoting the activation of signaling pathways required for lung cancer cell metastasis to multiple organ sites including brain and bone.

We found that ABL kinases promote metastasis by lung cancer cells harboring not only mutant EGFR but also mutant KRAS. Thus, ABL kinases may function as integrator kinases downstream of diverse oncogenic mutations. ABL kinases are activated downstream of multiple RTKs (6, 40). Following activation, the ABL kinases often promote phosphorylation of the activating RTK and engage in bidirectional

signaling that may result in decreased internalization of the receptor (41). Activation of ABL kinases in KRAS-mutant-expressing cells may also be mediated by RTK signaling, as mutant KRAS promotes expression of the EGFR ligand epiregulin, which binds to wild-type EGFR in these cells, thereby promoting autocrine cell growth and survival (42). Thus, activation of ABL kinases in lung cancer cells with EGFR or KRAS mutations can occur independently of *ABL* genomic alterations.

Following entry into the circulation, cancer cells must traverse the vasculature at distant organ sites to seed metastasis (25). Here we show, possibly for the first time, that ABL kinases are required for cancer cell extravasation. This finding is in contrast with a report showing that loss of *ABL2* does not affect extravasation of breast cancer cells (43). We previously reported that ABL kinases are required for metastatic colonization of breast cancer cells in bone (44). Thus, ABL kinases may regulate distinct steps in the metastatic cascade depending on the tumor cell type and the activation of cell-context-dependent signaling pathways. Extravasation is dependent on intercellular interactions between cancer cells, immune cells, and vascular endothelial cells (25). Multiple signaling pathways have been identified that regulate adhesive interactions between tumor and endothelial cells. ABL kinases have been shown to regulate chemokine-induced migration of T cells to sites of inflammation by activating the Rap1 and Rac1 GTPases, which regulate leukocyte adhesion, rolling, and transendothelial migration (45). Future studies are needed to dissect the mechanisms by which ABL kinases regulate extravasation and colonization of distal organ sites. These mechanisms may be dependent on the expression of survival factors such as survivin and Bcl-XL that function to protect cancer cells from apoptosis before or after extravasation. ABL kinases may also promote metastasis by increasing intercellular adhesion, thereby enhancing the formation of CTC clusters. This possibility is consistent with the finding that loss of both *ABL1* and *ABL2* disrupts cell-cell adhesion among fibroblasts and epithelial cells (46, 47). In this regard, CTC clusters have been reported to exhibit greater colonization efficiency by protecting cells from apoptosis and enhancing intercellular signaling within the heterogeneous cancer cells in the cluster (26, 48).

Mechanistically, we found that ABL kinases promote NSCLC metastasis in part through post-transcriptional regulation of the β -catenin and TAZ transcriptional coactivator proteins. Using GSEA of multiple databases we found that inactivation of the ABL kinases in NSCLC cells decreased the expression of the WNT/ β -catenin and TAZ pathway signatures. Interestingly, elevated expression of TAZ, but not YAP, has been reported in some NSCLC cell lines (31) and knockdown of TAZ inhibited lung tumor growth and metastasis (29, 31). We showed that expression of either activated β -catenin or TAZ mutants in *ABL1/ABL2* knockdown cells rescued metastatic activity. At the molecular level, inhibition of the ABL kinases enhanced the interaction of both β -catenin and TAZ proteins with the β -TrCP E3 ligase, leading to decreased β -catenin and TAZ protein stability. Our findings support a role for active ABL kinases in disrupting the interactions of β -catenin and TAZ with components of the destruction complex through inactivation of GSK3, thereby promoting β -catenin and TAZ protein stability, and enhanced nuclear localization and transcriptional activities in NSCLC cells. Previous reports showed interdependent regulation of β -catenin and TAZ/YAP signaling (49). We found that expression of some β -catenin target genes such as MYC and cyclin D1 and D3 was rescued by expression of active TAZ in lung cancer cells. Interestingly, YAP has been recently shown to promote extravasation of breast cancer cells in zebrafish and mouse models in part through upregulation of cytokine expression (50). Thus, ABL kinases may promote extravasation in part by activation of TAZ/YAP signaling.

Activation of β -catenin and TAZ pathways has been independently implicated in therapy resistance (51, 52). Among mechanisms of acquired resistance to EGFR inhibitors are amplification and mutation of the EGFR and other RTKs, as well as increased ligand-induced RTK signaling through autocrine or paracrine production of growth factors (53). Thus, targeting common downstream signaling mediators of multiple RTKs such as the ABL kinases might be an effective strategy for overcoming therapy resistance. Future studies are warranted to evaluate whether inactivation of the ABL kinases sensitizes therapy-resistant lung tumors to chemotherapy and/or targeted therapies. Allosteric ABL inhibitors are currently in clinical trials for the treatment of BCR-ABL-positive leukemia (<https://clinicaltrials.gov/show/NCT02081378>). Our data showing profound suppression of NSCLC metastasis by the ABL allosteric inhibitors in mice suggest that these compounds might be effective to treat metastatic NSCLC with a hyperactive ABL signature.

Methods

Cell culture. The human NSCLC cell line H358 was purchased from ATCC. PC9 parental and PC9-derived metastatic PC9M cells were gifts from Joan Massagué (Memorial Sloan-Kettering Cancer Center, New York, New York, USA). H460 parental and the H460-derived metastatic cell line M4M5 were provided by Fernando Lecanda (University of Navarra, Pamplona, Spain). All cells were maintained in RPMI 1640 (Life Technologies) supplemented with 10% fetal bovine serum (FBS, Life Technologies), 10 mM HEPES, 1 mM sodium pyruvate, and 0.2% glucose. H293T cells, a packaging cell line for virus production, were maintained in DMEM (Life Technologies) supplemented with 10% FBS. All cultures were maintained at 37°C in humidified air containing 5% CO₂.

RNAseq analysis. For RNAseq analysis, NSCLC cell lines H358, PC9, and PC9M were treated with or without GNF5 (8 μM for H358, 10 μM for PC9, and 20 μM for PC9M) for 72 hours. The same volume of DMSO was used for control samples. For depletion of ABL1/ABL2 proteins, PC9, PC9M, H460, and M4M5 cells were transduced with lentiviruses encoding either scrambled or ABL1/ABL2-specific shRNAs followed by FACS. Total RNA was isolated using the RNeasy kit (Qiagen); 1 μg total RNA input was used for each sample. Libraries were sequenced on an Illumina HiSeq 2000 sequencing system using 50-bp single-ended reads by the Duke University Genome Sequencing facility. RNAseq data were mapped to a reference genome (HG19) using Bowtie/Tophat. Reads were counted and differential expression between distinct experimental groups was quantified using Cuffdiff. Significant genes were extracted using R cummeRbund.

DNA plasmids. For ABL1/ABL2 knockdown, shRNA targeting sequences were as follows: scrambled shRNA (GGTGTATGGGCTACTATAGAA); ABL1 shRNA (GGTGTATGAGCTGCTAGAGAA); ABL2 shRNA 1 (CCTTATCTCACCCACTCTGAA); and ABL2 shRNA 2 (AGGTAATAAGTG-GCTCTGAG) (54). Active ABL1 (ABL1-PP) and ABL2 (ABL2-PP) in the MigR1 vector were generated by mutating 2 proline residues in the interlinker region to glutamate as described previously (41). CTNNB1 (S33A, S37A, T41A, S45A) in pLX304 (catalog 42561) and pLenti-EF-FH-TAZ-ires-blast (catalog 52083) were obtained from Addgene. Plasmids pLVX-Tet-On vector and pLVX-TP-3F-TAZ4SA (S66A, S89A, S117A and S311A) were provided by Xaralabos Varelas (Boston University, Boston, Massachusetts, USA) (55). YAP/TAZ-responsive luciferase reporter (8xGTIIIC-luciferase, catalog 34615) and β-catenin-responsive luciferase reporter (7xTcf-FFluc, catalog 24308) were obtained from Addgene. pCMV-β-galactosidase DNA was provided by Donald McDonnell (Duke University). Inducible shRNA specific for ABL1 was constructed in the pLKO-Tet-On vector.

Viral transduction. Retroviral packaging DNAs pCMV-Gag-Pol and pCMV-VSVG were used for ABL1-PP and ABL2-PP (in MigR1 vector) transduction, and lentiviral packaging DNAs pMDL, pCMV-VSVG, and pRSV-REV were used for shRNAs and BC4SA and TAZ4SA transduction. 293T cells were transfected with packaging DNAs along with corresponding DNAs using FuGENE6 reagent (Promega). Culture supernatants containing retroviruses or lentiviruses were collected and filtered 24 hours and 48 hours after transfection and used for transducing NSCLC cells in the presence of 8 μg/ml Polybrene (Sigma-Aldrich). Cells transduced with retroviruses encoding active ABL1/ABL2 or transduced with lentiviruses encoding shRNAs were selected by GFP FACS. PC9 cells transduced with lentiviruses encoding BC4SA were selected with blasticidin (5 μg/ml), and PC9 cells transduced with lentiviruses encoding pLVX-Tet-On and TAZ4SA were selected with G418 (100 μg/ml) and puromycin (1 μg/ml).

NSCLC tumor metastasis and analysis. Age-matched female athymic NCr nu/nu mice (5–8 weeks old) were used for all experiments. Cells were transduced with pFU-luciferase-tomato DNA. For depletion of ABL1/ABL2 proteins, PC9, PC9M, H460, and M4M5 cells were transduced with either scrambled or ABL1/ABL2-specific shRNAs followed by FACS. For intracardiac injections, PC9 (4 × 10⁵), PC9M (2 × 10⁵), H460 (1 × 10⁵), and M4M5 (2 × 10⁵) cells were injected into the left cardiac ventricle using 30-gauge needles. The allosteric inhibitor GNF5 was synthesized by the Duke University Small Molecule Synthesis Facility. GNF5 was prepared either in 0.5% methyl cellulose/0.5% Tween-80 (10 mg/ml) for oral gavage at 100 mg/kg twice daily or in DMSO/peanut oil (1:9, 50 mg/ml) for intraperitoneal injection at 50 mg/kg once per day. Control mice were treated with the same solvents used to dissolve GNF5. Mice were anesthetized with isoflurane before injection and imaged by BLI. GNF5 was used at 5 to 10 μM for PC9 cells, and at 10 to 20 μM for PC9M, H460, and M4M5 cells in vitro.

NSCLC cell extravasation. PC9 or PC9M cells transduced with either scrambled or ABL1/ABL2-specific shRNAs were labeled with Celltracker Green CMFDA (Thermo Fisher Scientific). Cells (5 × 10⁵) were injected into the tail vein of nude mice. Extravasation into the lung parenchyma was quantified 24 hours after injection.

Rhodamine-conjugated lectin was injected into the tail vein 5 minutes before euthanasia to label the vessels. Lungs were inflated and fixed in 4% paraformaldehyde in PBS. Lung lobes were embedded in agarose and sectioned with a vibratome. Extravasated cells were analyzed with a Leica SP5 inverted confocal microscope. We used a Zeiss Axio Imager Z2 upright microscope to evaluate the numbers of labeled green cells in each entire lung section. For short time point analysis, we collected lungs 2 hours after tail vein injection of tumor cells. Lung lobes were cut into small pieces in PBS/0.3% Triton X-100 followed by immunostaining with anti-CD31 antibody to visualize the blood vessels. Images were obtained using a Leica SP5 inverted confocal microscope.

Transient transfection and luciferase reporter assay. PC9 cells (1×10^4) plated in 96-well plates in triplicate were transfected with TAZ-responsive luciferase reporter (8xGTTC-luciferase) or β -catenin-responsive luciferase reporter (7xTcf-FFluc), along with β -galactosidase using FuGENE6 reagent in Opti-MEM Reduced Serum Medium (Life Technologies). After 20 hours, cells were treated with or without GNF5 for another 24 hours before analyzing using a Dual-Light System (Applied Biosystems).

Western immunoblotting. Cells were lysed in RIPA buffer (50 mM Tris-HCl, pH 7.5, 150 mM NaCl, 1% Triton X-100, 0.1% SDS, and 0.5% sodium deoxycholate with protease/phosphatase inhibitors). Cell debris was removed by microcentrifugation, and protein concentration was quantified using the DC Protein Assay (Bio-Rad Laboratories). Equal amounts of protein were separated by SDS/PAGE, transferred onto nitrocellulose membranes, and probed with the indicated antibodies. Samples were either run in the same gel and transferred to the membrane, which was then cut into several strips to blot for proteins with different molecular weights with specific antibodies, or alternatively, the same samples were run contemporaneously in parallel gels to blot for several proteins, some of which have the same molecular weights. We have indicated in the figure legends when the same experimental samples were run in different gels. To concentrate secreted proteins from the culture supernatant, Amicon Ultra 0.5-ml centrifugal filters (Ultracell-10K) were used following the manufacturer's instructions. All antibodies used are listed in Supplemental Table 2.

Nuclear/cytosolic fractionation. Cells were washed with PBS and lysed in Buffer A (10 mM HEPES, pH 7.9, 10 mM KCl, 0.1 mM EDTA, 0.1 mM EGTA, 0.6% NP40, and Protease Inhibitor Cocktail [Sigma-Aldrich]). Lysates were centrifuged and the supernatant was collected as the cytosolic fraction. After washing the pellets several times using Buffer A, pellets were resuspended in Buffer C (20 mM HEPES pH 7.9, 25% glycerol, 0.4 M NaCl, 1 mM EDTA, and 1 mM EGTA plus Protease Inhibitor Cocktail) and incubated at 4°C for 20 minutes with gentle shaking. Lysates were centrifuged and the supernatant was collected as the nuclear fraction. Proteins in both fractions were quantified and analyzed by Western blotting.

Immunoprecipitation and ABL kinase assay. Cells lysed in NP40 buffer (20 mM Tris-HCl, pH 8, 137 mM NaCl, 1% NP40 and 2 mM EDTA plus protease/phosphatase inhibitors) were incubated with either anti-TAZ or anti- β -catenin (BD Biosciences) antibodies overnight at 4°C with agitation. Protein A/G Plus-Agarose (Santa Cruz Biotechnology) was used to pull down the complex. After washing thoroughly with lysis buffer, samples were boiled, separated by SDS/PAGE, and membranes probed with the indicated antibodies. For PC9 cells expressing Flag-tagged TAZ, immunoprecipitation was performed using Anti-Flag M2 Affinity Gel (Sigma-Aldrich). For ABL kinase assays, ABL proteins were immunoprecipitated and incubated with glutathione *S*-transferase-tagged CRK in the presence of 1 μ M ATP for 30 minutes. Phosphorylation of CRK was assessed using phospho-specific (Y221) antibody (Cell Signaling Technology).

Immunohistochemistry and immunofluorescence staining. For immunohistochemistry, sections of human lung cancer samples were obtained from the Biospecimen Repository and Processing Core, a shared resource of the Duke University School of Medicine and Duke Cancer Institute. Paraffin sections (5 μ m) underwent 10 mM sodium citrate antigen retrieval and were then stained with the following primary antibodies: rabbit anti- β -catenin (Cell Signaling Technology), rabbit anti-survivin (Cell Signaling Technology), rabbit anti-TAZ (Abcam), and rabbit anti-S100A4 (Abcam). Alexa Fluor-coupled secondary antibodies (Invitrogen) were used at 1:400 dilution. All images were captured on an Axio Imager D10 (Carl Zeiss) with a 40 \times /0.75 EC Plan-Neofluar objective lens.

For immunofluorescence staining, cells were plated in 8-well chamber slides (Thermo Fisher Scientific) and were stained with either anti-TAZ (BD Biosciences) or anti- β -catenin antibodies (Abcam) as directed by the manufacturer's instructions. Appropriate Alexa Fluor-conjugated secondary antibodies (Santa Cruz Biotechnology) were used followed by Hoechst (Molecular Probes) staining to identify the nuclei. Fluorescence images were acquired using the Carl Zeiss MicroImaging Axiovert 200M.

Cell viability and growth assay and soft agar colony formation assay. For cell viability and growth in 2-dimensional cultures, cells were seeded in 96-well plates in triplicate and measured each day using CellTiter-Glo

(Promega). For colony assays, cell culture wells were coated with 0.8% SeaPlaque Agarose (Lonza), and 800 cells (for 48-well plates) in 0.4% agarose with 1× medium were then plated in the wells in triplicate. Colonies (size > 100 μm) were visualized at ×2.5 magnification after 15 to 25 days, and multiple fields of nonoverlapping area were used for quantification.

NCLC tumor xenografts. H460 cells harboring doxycycline-inducible ABL1-specific shRNA were injected subcutaneously into nude mice. Once tumors reached ~100 mm³ mice were treated with doxycycline (1 mg/ml) in the drinking water. Cells harboring nontargeting shRNA (sh-NT) were used as controls. Tumors were measured before and after doxycycline induction. Tumors were isolated after 13 days of induction and were weighed.

Real-time RT-PCR. RNA was isolated from cancer cells using the RNeasy RNA isolation kit (Qiagen), and cDNA was synthesized using oligo(dT) primer and M-MLV reverse transcriptase (Invitrogen). Real-time PCR was performed using iQ SYBR Green Supermix (Bio-Rad). Primers used for this study are listed in Supplemental Table 3. Analysis was performed using a Bio-Rad CFX384 real-time machine and CFX Manager software. PCR assays were performed in triplicate. Expression levels of each gene were normalized to the expression of the *GAPDH* housekeeping control gene.

Statistics. Statistical analyses were performed using GraphPad Prism 5 software. Comparisons of 2 groups were performed using Student's *t* tests (unpaired, 2-tailed). For comparison of 2 groups' survival, *P* values were calculated using a log-rank (Mantel-Cox) test. Comparisons involving multiple groups were evaluated using 1-way ANOVA, followed by Tukey's honest significant difference test. For all tests, a *P* value less than 0.05 was considered statistically significant.

Study approval. All procedures involving mice were approved and performed following the guidelines of the IACUC of Duke University Division of Laboratory Animal Resources. All experiments using human tissues were approved by the Duke University IRB, protocol ID Pro00076362, effective 8/24/16.

RNAseq accession numbers. The NCBI Gene Expression Omnibus accession number for RNAseq data reported in this paper is GSE77422.

Author contributions

JJG and AMP conceived the study, generated hypotheses, designed the experiments, and analyzed the data. JJG performed the experiments. MWO provided clinical samples and intellectual advice. CR provided technical expertise and contributed to mouse experiments. XX performed immunohistochemistry on patient-derived samples. JW provided assistance for bioinformatics analysis. JJG and AMP wrote the manuscript.

Acknowledgments

We thank D. Neil Hayes (University of North Carolina at Chapel Hill, Lineberger Comprehensive Cancer Center, Chapel Hill, North Carolina, USA) for expert advice on analysis of overall survival of lung cancer patients with active ABL signature. We also thank Joan Massagué (Memorial Sloan-Kettering) and Fernando Lecanda (University of Navarra) for NSCLC cell lines. We are grateful to Xaralabos Varelas (Boston University) for providing TAZ-mutant plasmid DNAs. We thank Aaditya Khatri and Emileigh Greuber for technical assistance. We acknowledge and thank the Biospecimen Repository and Processing Core (BRPC), a shared resource of the Duke University School of Medicine and Duke Cancer Institute, for providing access to the human biospecimens used under IRB oversight in this work. The BRPC receives support from the P30 Cancer Center Support Grant (P30 CA014236). We thank the Duke Cancer Center Shared Resource of Optical Molecular Imaging and Analysis, Light Microscopy Core Facility, Flow Cytometry and Histology and Microscopy Core facility. This work was supported by NIH Grant R01 CA195549 (to A.M.P.), Free to Breathe Metastasis Research Grant (to A.M.P. and M.W.O.), Uniting Against Lung Cancer Grant (to A.M.P.), AATS Graham Foundation Research Grant (to M.W.O.), and NIH Grant R21 CA201486 (to M.W.O.).

Address correspondence to: Ann Marie Pendergast, Department of Pharmacology and Cancer Biology, Duke University School of Medicine, Box 3813, Durham, North Carolina 27710, USA. Phone: 919.681.8086; E-mail: ann.pendergast@duke.edu.

1. Li T, Kung HJ, Mack PC, Gandara DR. Genotyping and genomic profiling of non-small-cell lung cancer: implications for current and future therapies. *J Clin Oncol*. 2013;31(8):1039–1049.
2. Mascaux C, et al. The role of RAS oncogene in survival of patients with lung cancer: a systematic review of the literature with meta-analysis. *Br J Cancer*. 2005;92(1):131–139.
3. Coleman RE. Clinical features of metastatic bone disease and risk of skeletal morbidity. *Clin Cancer Res*. 2006;12(20 Pt 2):6243s–6249s.
4. Siegel R, Naishadham D, Jemal A. Cancer statistics, 2013. *CA Cancer J Clin*. 2013;63(1):11–30.
5. Eichler AF, Chung E, Kodack DP, Loeffler JS, Fukumura D, Jain RK. The biology of brain metastases—translation to new therapies. *Nat Rev Clin Oncol*. 2011;8(6):344–356.
6. Wang J, Pendergast AM. The emerging role of ABL kinases in solid tumors. *Trends Cancer*. 2015;1(2):110–123.
7. Cancer Genome Atlas Research Network. Comprehensive molecular profiling of lung adenocarcinoma. *Nature*. 2014;511(7511):543–550.
8. Sos ML, et al. Predicting drug susceptibility of non-small cell lung cancers based on genetic lesions. *J Clin Invest*. 2009;119(6):1727–1740.
9. Testoni E, et al. Somatic mutated ABL1 is an actionable and essential NSCLC survival gene. *EMBO Mol Med*. 2016;8(2):105–116.
10. Zhou S, et al. Overexpression of c-Abl predicts unfavorable outcome in epithelial ovarian cancer. *Gynecol Oncol*. 2013;131(1):69–76.
11. Rikova K, et al. Global survey of phosphotyrosine signaling identifies oncogenic kinases in lung cancer. *Cell*. 2007;131(6):1190–1203.
12. Hess KR, et al. Metastatic patterns in adenocarcinoma. *Cancer*. 2006;106(7):1624–1633.
13. Massagué J, Obenauf AC. Metastatic colonization by circulating tumour cells. *Nature*. 2016;529(7586):298–306.
14. Nguyen DX, Bos PD, Massagué J. Metastasis: from dissemination to organ-specific colonization. *Nat Rev Cancer*. 2009;9(4):274–284.
15. Nguyen DX, et al. WNT/TCF signaling through LEF1 and HOXB9 mediates lung adenocarcinoma metastasis. *Cell*. 2009;138(1):51–62.
16. Valencia K, et al. Inhibition of collagen receptor discoidin domain receptor-1 (DDR1) reduces cell survival, homing, and colonization in lung cancer bone metastasis. *Clin Cancer Res*. 2012;18(4):969–980.
17. Vicent S, et al. A novel lung cancer signature mediates metastatic bone colonization by a dual mechanism. *Cancer Res*. 2008;68(7):2275–2285.
18. Subramanian A, et al. Gene set enrichment analysis: a knowledge-based approach for interpreting genome-wide expression profiles. *Proc Natl Acad Sci USA*. 2005;102(43):15545–15550.
19. Dat le T, et al. Identification of genes potentially involved in bone metastasis by genome-wide gene expression profile analysis of non-small cell lung cancer in mice. *Int J Oncol*. 2012;40(5):1455–1469.
20. Kikuchi T, et al. Expression profiles of metastatic brain tumor from lung adenocarcinomas on cDNA microarray. *Int J Oncol*. 2006;28(4):799–805.
21. Luis-Ravelo D, et al. A gene signature of bone metastatic colonization sensitizes for tumor-induced osteolysis and predicts survival in lung cancer. *Oncogene*. 2014;33(43):5090–5099.
22. Zohrabian VM, et al. Gene expression profiling of metastatic brain cancer. *Oncol Rep*. 2007;18(2):321–328.
23. Zhang J, et al. Targeting Bcr-Abl by combining allosteric with ATP-binding-site inhibitors. *Nature*. 2010;463(7280):501–506.
24. Packer LM, et al. Nilotinib and MEK inhibitors induce synthetic lethality through paradoxical activation of RAF in drug-resistant chronic myeloid leukemia. *Cancer Cell*. 2011;20(6):715–727.
25. Reymond N, d'Água BB, Ridley AJ. Crossing the endothelial barrier during metastasis. *Nat Rev Cancer*. 2013;13(12):858–870.
26. Aceto N, et al. Circulating tumor cell clusters are oligoclonal precursors of breast cancer metastasis. *Cell*. 2014;158(5):1110–1122.
27. Noguchi S, et al. An integrative analysis of the tumorigenic role of TAZ in human non-small cell lung cancer. *Clin Cancer Res*. 2014;20(17):4660–4672.
28. Ziegler S, et al. Novel target genes of the Wnt pathway and statistical insights into Wnt target promoter regulation. *FEBS J*. 2005;272(7):1600–1615.
29. Lau AN, et al. Tumor-propagating cells and Yap/Taz activity contribute to lung tumor progression and metastasis. *EMBO J*. 2014;33(5):468–481.
30. Stewart DJ. Wnt signaling pathway in non-small cell lung cancer. *J Natl Cancer Inst*. 2014;106(1):djt356.
31. Zhou Z, Hao Y, Liu N, Raptis L, Tsao MS, Yang X. TAZ is a novel oncogene in non-small cell lung cancer. *Oncogene*. 2011;30(18):2181–2186.
32. MacDonald BT, Tamai K, He X. Wnt/beta-catenin signaling: components, mechanisms, and diseases. *Dev Cell*. 2009;17(1):9–26.
33. Park HW, et al. Alternative Wnt signaling activates YAP/TAZ. *Cell*. 2015;162(4):780–794.
34. Meng Z, Moroishi T, Guan KL. Mechanisms of Hippo pathway regulation. *Genes Dev*. 2016;30(1):1–17.
35. Taurin S, Sandbo N, Qin Y, Browning D, Dulin NO. Phosphorylation of beta-catenin by cyclic AMP-dependent protein kinase. *J Biol Chem*. 2006;281(15):9971–9976.
36. Ruvolo PP, et al. Phosphorylation of GSK3 α / β correlates with activation of AKT and is prognostic for poor overall survival in acute myeloid leukemia patients. *BBA Clin*. 2015;4:59–68.
37. Harvey KF, Zhang X, Thomas DM. The Hippo pathway and human cancer. *Nat Rev Cancer*. 2013;13(4):246–257.
38. Lei QY, et al. TAZ promotes cell proliferation and epithelial-mesenchymal transition and is inhibited by the hippo pathway. *Mol Cell Biol*. 2008;28(7):2426–2436.
39. Huang W, et al. The N-terminal phosphodegron targets TAZ/WWTR1 protein for SCF β -TrCP-dependent degradation in response to phosphatidylinositol 3-kinase inhibition. *J Biol Chem*. 2012;287(31):26245–26253.
40. Khatri A, Wang J, Pendergast AM. Multifunctional Abl kinases in health and disease. *J Cell Sci*. 2016;129(1):9–16.
41. Plattner R, Koleske AJ, Kazlauskas A, Pendergast AM. Bidirectional signaling links the Abelson kinases to the platelet-derived growth factor receptor. *Mol Cell Biol*. 2004;24(6):2573–2583.
42. Sunaga N, et al. Oncogenic KRAS-induced epi-regulin overexpression contributes to aggressive phenotype and is a promising

- therapeutic target in non-small-cell lung cancer. *Oncogene*. 2013;32(34):4034–4042.
43. Gil-Henn H, Patsialou A, Wang Y, Warren MS, Condeelis JS, Koleske AJ. Arg/Abl2 promotes invasion and attenuates proliferation of breast cancer in vivo. *Oncogene*. 2013;32(21):2622–2630.
44. Wang J, Rouse C, Jasper JS, Pendergast AM. ABL kinases promote breast cancer osteolytic metastasis by modulating tumor-bone interactions through TAZ and STAT5 signaling. *Sci Signal*. 2016;9(413):ra12.
45. Gu JJ, Lavau CP, Pugacheva E, Soderblom EJ, Moseley MA, Pendergast AM. Abl family kinases modulate T cell-mediated inflammation and chemokine-induced migration through the adaptor HEF1 and the GTPase Rap1. *Sci Signal*. 2012;5(233):ra51.
46. Li R, Pendergast AM. Arg kinase regulates epithelial cell polarity by targeting β 1-integrin and small GTPase pathways. *Curr Biol*. 2011;21(18):1534–1542.
47. Zandy NL, Playford M, Pendergast AM. Abl tyrosine kinases regulate cell-cell adhesion through Rho GTPases. *Proc Natl Acad Sci USA*. 2007;104(45):17686–17691.
48. Yu M, et al. Circulating breast tumor cells exhibit dynamic changes in epithelial and mesenchymal composition. *Science*. 2013;339(6119):580–584.
49. Azzolin L, et al. YAP/TAZ incorporation in the β -catenin destruction complex orchestrates the Wnt response. *Cell*. 2014;158(1):157–170.
50. Sharif GM, et al. Cell growth density modulates cancer cell vascular invasion via Hippo pathway activity and CXCR2 signaling. *Oncogene*. 2015;34(48):5879–5889.
51. Bartucci M, et al. TAZ is required for metastatic activity and chemoresistance of breast cancer stem cells. *Oncogene*. 2015;34(6):681–690.
52. Spranger S, Bao R, Gajewski TF. Melanoma-intrinsic β -catenin signalling prevents anti-tumour immunity. *Nature*. 2015;523(7559):231–235.
53. Wilson TR, et al. Widespread potential for growth-factor-driven resistance to anticancer kinase inhibitors. *Nature*. 2012;487(7408):505–509.
54. Chislock EM, Ring C, Pendergast AM. Abl kinases are required for vascular function, Tie2 expression, and angiopoietin-1-mediated survival. *Proc Natl Acad Sci USA*. 2013;110(30):12432–12437.
55. Varelas X. The Hippo pathway effectors TAZ and YAP in development, homeostasis and disease. *Development*. 2014;141(8):1614–1626.